

## Cluster Populations in A115 and A2283

Karl D. Rakos

Institute for Astronomy, University of Vienna, A-1180, Wien, Austria; rakosch@astro1.ast.univie.ac.at

James M. Schombert

Department of Physics, University of Oregon, Eugene, OR 97403; js@abyss.uoregon.edu

Andrew P. Odell

Department of Physics and Astronomy, Northern Arizona University, Box 6010, Flagstaff, AZ 86011; andy.odell@nau.edu

Susanna Steindling

Wise Observatory and the School of Physics and Astronomy, Tel Aviv University, Tel Aviv, Israel; susan@wise1.tau.ac.il

### ABSTRACT

This paper presents four color narrow-band photometry of clusters A115 ( $z = 0.191$ ) and A2283 ( $z = 0.182$ ) in order to follow the star formation history of various galaxy types. Although located at similar redshifts, the two clusters display very different fractions of blue galaxies (i.e. the Butcher-Oemler effect,  $f_B = 0.13$  for A115,  $f_B = 0.30$  for A2283). A system of photometric classification is applied to the cluster members that divides the cluster population into four classes based on their recent levels of star formation. It is shown that the blue population of each cluster is primarily composed of normal starforming ( $\text{SFR} < 1M_{\odot} \text{ yrs}^{-1}$ ) galaxies at the high luminosity end, but with an increasing contribution from a dwarf starburst population below  $M_{5500} = -20$ . This dwarf starburst population appears to be the same population of low mass galaxies identified in recent HST imaging (Koo *et al.* 1997), possible progenitors to present-day cluster dwarf ellipticals, irregulars and BCD's. Deviations in the color-magnitude relationship for the red galaxies in each cluster suggest that a population of blue S0's is evolving into present-day S0 colors at this epoch. The radial distribution of the blue population supports the prediction of galaxy harassment mechanisms for tidally induced star formation operating on an infalling set of gas-rich galaxies.

### 1. INTRODUCTION

The investigation of the blue and red populations in rich clusters have been our most lucrative glimpse into the evolution of galaxies. The search for changes in the stellar population of galaxies has mostly focused on clusters of galaxies due to their high visibility and ease of cataloging rich clusters even at distant redshifts. However, the gravitational clumping of a cluster also minimizes the effort required for distance determination where the measurement of a few of the brightest galaxies provides the redshift for the entire cluster. Attention concerning recent and rapid evolution has been diverted in the past decade to field galaxies (Tyson 1988), and the dilemma of the blue field population. However, clusters are the sites of numerous dramatic evolutionary effects, such as galaxy cannibalism (Moore *et al.* 1996) and the Butcher-Oemler population (Oemler, Dressler and Butcher 1997). In addition, cluster populations are key to understanding galaxy characteristics since they cover not only a full range of galaxy masses (from giants to dwarfs) but also the full range of Hubble types and intrinsic density (e.g. surface brightness) that are missing from field populations.

In a series of papers extending over the last 12 years (Rakos *et al.* 1988, 1991, 1995, 1996, 1997, 1999), we have used a narrow band filter system to perform photometry of galaxies in rich clusters for redshifts ranging from 0.2 to 1. Our studies have differed from previous photometry of distant clusters by the use of a color system surrounding the 4000Å break (the Strömgren *uvby* system) and modified such that the filters are “redshifted” to the cluster of galaxies in consideration. This method results in effectively no k-corrections and allows discrimination between cluster membership based on spectrophotometric criteria. We call our modified system *uz, vz, bz, yz* to distinguish it from the original *uvby* Strömgren system and we believe we have demonstrated that these color indices are a profitable tool for investigating color evolution of both the red and blue populations in clusters of galaxies.

In an previous exploratory paper (Rakos, Maindl and Schombert 1996, hereafter RMS96), the modified *uz, vz, bz, yz* Strömgren system was used to develop a photometric classification scheme based on the recent star formation history of a galaxy. From the *mz* color index ( $mz = (vz - bz) - (bz - yz)$ ), the classification technique was shown to be extremely successful at discriminating normal starforming galaxies (spirals) and starburst galaxies despite the presence of heavy reddening. Rakos *et al.* (1996, 1997) applied this technique to the members of the blue population in several clusters of intermediate redshift ( $0.2 < z < 0.6$ ) and demonstrated that many of the cluster members have strong signatures of star formation activity. An extreme example is CL0317+1521 at  $z = 0.583$  which has a blue fraction of  $f_B = 0.60$  and which 42% of the blue population have  $mz < -0.2$ , the photometric signature for a starburst. Deep photometry of the cluster A2317 ( $z = 0.211$ , Rakos, Odell and Schombert 1997) demonstrated that the ratio of the blue population to red population has a strong dependence on luminosity, such that blue galaxies dominate the very brightest and very faintest galaxies in the cluster. In contrast to the bright blue galaxies, the fraction of galaxies displaying the signatures of a starburst increases towards the faint end of the luminosity function, a dwarf starburst population first suggested by Koo *et al.* (1997).

The origin of this dwarf starburst population remains an enigma. Tidal interactions are frequently invoked as an explanation for the high fraction of starburst galaxies in Butcher-Oemler clusters (Dressler *et al.* 1994, Couch *et al.* 1994). If the same phenomenon acts on the low mass galaxies, then these starburst systems would have their origin as gas-rich dwarf galaxies who have had a short, but intense, tidally induced episode of star formation which would quickly exhaust their limited gas supply. It should be noted, however, that the orbits of cluster galaxies are primarily radial (Bothun and Schombert 1990), and the typical velocities into the dense cluster core are high. This makes any encounter extremely short-lived, with little impulse being transferred as is required to shock the incumbent molecular clouds into a nuclear starburst. The galaxy harassment mechanism (Moore *et al.* 1996) emphasizes the influence of the cluster tidal field and the more powerful impulse encounters with individual central galaxies at the cluster edges. These two processes can then conspire raise the luminosity of cluster dwarfs, increase their visibility and, thus, their detectability.

To further explore the behavior of the red E/S0's, blue Butcher-Oemler galaxies and the newly detected dwarf starburst population, we began a program of obtaining deeper photometry then our previous work on intermediate redshift clusters. Our goal in this study is to 1) illuminate the types of galaxies involved in the Butcher-Oemler effect, 2) determine the dominance of the blue galaxies to the cluster luminosity function, 3) examine the spatial extent of the blue and red population, and 4) determine the existence and characteristics of the dwarf starburst population in other blue clusters. In order to maintain a correct timescale to stellar population models, calibrated to globular cluster ages, values of  $H_o = 50$  km sec $^{-1}$  Mpc $^{-1}$  and  $q_o = 0$  are used throughout this paper.

## 2. OBSERVATIONS

### 2.1. Cluster Sample

To determine if the results for A2317 were accidental, we have expanded our program to three clusters at similar redshifts; A115 ( $z = 0.191$ ), A2283 ( $z = 0.182$ ) and A2218 ( $z = 0.180$ ). Table 1 shows the cluster coordinates (1950.0), the Bautz-Morgan classification and the background corrected count  $C$  in the magnitude range  $m_3 + 3$  (Abell richness). A115 and A2283 are similar to A2317 in richness. A2218 is, on the other hand, one of the richest clusters in the Abell catalog and contains a large cD galaxy in its center which extends over more than 180 kpc (Wang and Ulmer 1997). A115 is also a known binary cluster (Beers, Huchra and Geller 1983) which is normally associated with a dynamically young system. A115 was also studied by our group in a previous paper (Rakos, Fiala and Schombert 1988); however, only 53 galaxies were measured at that time. This paper presents new results for A115 and A2283. The data for A2218 will be presented in a later paper (Rakos, Dominis and Steindling 2000).

The observing procedure and reduction used herein is similar to that described in Rakos and Schombert (1995). The observations of A115 were taken with 90-inch Steward Observatory telescope using 800x1200 pixel CCD and a focal reducer with 600 arcsec circular unvignetted field at a f/9 input beam. A2283 was observed with the 4m KPNO PFCCD Te1K, the 90-inch Steward telescope in direct mode plus 2K CCD and the 1m Wise telescope in Israel using 1K TEK CCD. The field size for the Wise telescope is 10 arcmin square. Calibration to the  $uz, vz, bz, yz$  system used spectrophotometric standards (Massey *et al.* 1988). Colors and magnitudes were measured using IRAF APPHOT and are based on metric apertures set at 32 kpc (9 arcsecs for A115 and A2283) for cosmological parameters of  $H_o = 50 \text{ km sec}^{-1} \text{ Mpc}^{-1}$  and  $q_o = 0$ . Our typical internal errors were 0.05 mag in colors at the bright end of the sample and 0.1 mag for the faint end. No corrections for Galactic extinction were made due to the high latitude of the clusters. All the photometry ( $uz - vz$ ,  $bz - yz$ ,  $vz - yz$  and  $mz$ ) is available at the narrow band photometry web site ([zebu.uoregon.edu/~js/narrow](http://zebu.uoregon.edu/~js/narrow)).

Photometry using 32 kpc apertures was performed on the final, co-added frames. Objects were selected based on detection in all four filters at the  $3\sigma$  level. In addition to the colors, the  $yz$  filter values can be converted to  $m_{5500}$ . The Strömgren system was originally designed only as a color system; however, the  $yz$  filter is centered on 5500Å and it is possible to link the  $yz$  flux to a photon magnitude, such as the AB79 system of Oke and Gunn 1983, through the use of spectrophotometric standards. This procedure was described in detail in Rakos, Fiala and Schombert (1988) and is used to determine the  $m_{5500}$  values for all the cluster members. Typical errors were 0.02 mag for the brightest cluster members to 0.08 mag for objects below  $m_{5500} = 20$ . Incompleteness of both clusters is evident below  $M_{5500} = -20$ , the faintest objects are  $M_{5500} = -19$ .

### 2.2. Cluster Membership

Each of the filters used for this study are approximately 200Å wide and were specially designed so that their central wavelengths matches the rest frame of the cluster. This provides a photometric method of determining cluster membership, without the use of redshift information, due to the unique shape of any galaxy's spectra around the 4000Å break. Our method is fully discussed in Rakos, Schombert and Kreidl (1991) and Fiala, Rakos and Stockton (1986), but a brief discussion follows.

Figure 1 displays the changes in color indices for a standard elliptical profile (NGC 3379, Kennicutt

1992) and a starforming disk (NGC 6643, Kennicutt 1992) as a function of redshift. Since the 4000Å break brackets the  $uz$  and  $vz$  filters, sharp blue  $vz - yz$  colors are seen for low redshift objects (relative to the cluster redshift, i.e. foreground) and red  $bz - yz$  colors are found for high redshift objects (background).

Our procedure to determine cluster membership is to use the color information provided by the  $mz$ ,  $vz - yz$  and  $bz - yz$  indices to measure a distance from the normal galaxy templates (see Rakos, Schombert and Maindl 1996). Any object more than  $3\sigma$  from the mean relationships is eliminated from the sample. As expected, a majority of the rejected objects are too red (background), but the criteria also eliminates foreground stars. While there could be contamination from poor S/N galaxies, whose erroneous colors place them within the  $3\sigma$  boundaries. However, these objects are eliminated by our photometric quality criteria (typically  $\sigma < 0.07$  mag, see below).

To test this procedure for A115, redshifts were extracted from NED. Within the 10 arcmin field of A115, 14 galaxies with redshifts are found, 12 at the cluster redshift ( $z = 0.191$ ) and two at a foreground redshift of 14,388 and 14,307 km sec $^{-1}$ . Ten of the twelve cluster galaxies were correctly identified by the photometric criteria, two others were eliminated due to poor S/N. The two foreground galaxies were correctly eliminated as non-cluster members by their  $mz$  indices.

In A2218, five galaxies have redshifts, two cluster members and three foreground objects. As with A115, all three foreground objects were eliminated by the photometric criteria. One of the cluster members was identified, the other was too close to a bright, nearby galaxy for proper measurement. Combined with the A115 results, we believe this to validate our procedure, at least for the brighter cluster members. We only have numerical simulations for the fainter cluster members.

### 2.3. Photometric Classification

Before the advent of 2D photometry and spectroscopy, galaxies were understood by their morphological appearance and integrated colors. Star formation, in particular, was estimated based on the size and number of H II regions rather than the number of ionizing photons as produced by a set number of O and B stars. Currently, the morphological appearance of a galaxy has become a secondary parameter as the field of galaxy evolution has become more concerned with the actual star formation history of galaxies based on fits to spectrophotometric models, rather than the inferred history based on our conception of how star formation and galaxy appearance are related. Although there is a strong correlation between the current star formation rate and the morphological class of a galaxy, most of the questions arising in high redshift cluster studies will involve the underlying stellar and gas components of a galaxy, not its appearance.

Classification by colors or spectral type have their origin in the Morgan system (Morgan and Mayall 1957). Although primitive in its information, the Morgan system was key to developing an understanding of the morphological type of a galaxy as it relates to the state of its underlying stellar population. Modern studies have successfully applied spectrophotometric classification to starforming and starburst systems in distant clusters (Poggianti *et al.* 1999).

The exact classification procedure for our Strömgren filters was discussed in RMS96, but the following is a brief review. For the purposes of classification, the galaxy types in clusters are basically divided into four categories based on their color indices as they reflect into current and recent star formation. The four classes are 1) a passive, non-starforming object (presumably the counterpart to present-day ellipticals and S0's, at least in terms of the current star formation rate (SFR), if not the integrated past SFR), 2) a normal

starforming object (with an SFR between 0.1 and  $1 M_{\odot}$  yrs $^{-1}$  and standard values for the IMF, Kennicutt 1998) which can be associated with present-day spirals, 3) an object with anomalous colors that correspond to a region in the two-color plane occupied by starburst objects (i.e. SFRs greater than  $1 M_{\odot}$  yrs $^{-1}$ ) and 4) objects with a non-thermal component to their luminosity that is associated with Seyfert activity.

This classification system is not exact, there are several transition regions that produce an ambiguous assignment of the state of the stellar population. The three most serious are the regions occupied by early-type spirals, low luminosity Seyfert galaxies and weak or post-starburst systems. Early-type spirals are found to overlap with the passive or E/S0 region of photometric space. This is not surprising since our system emphasizes the integrated color of a galaxy, and the large bulge component of early-type galaxies dominates the colors over a minor disk component. The impact of early-type spirals is minimized within the goals of our work since we can easily group galaxies with short gas depletion rates (ellipticals, S0's and early-type spirals) into the same class when the focus is star formation rates.

The Seyfert classification overlaps with normal spirals depending on the ratio of the amount of light from the AGN versus the galaxy stellar disk. Most Seyfert galaxies are spiral (Ho, Filippenko and Sargent 1997), and heavily weighted towards late-types, in agreement with the model that AGN luminosity is correlated with the ability to fuel the central engine with HI gas. Since a global color measurement will overemphasize the contribution from normal starlight with respect to non-thermal emission, AGN colors will typically scatter towards the normal spiral sequence in multi-color space. Thus, when interpreting the fraction of Seyferts in our cluster sample, we must place the caveat that this fraction represents the number of ‘extreme’ Seyferts, i.e. ones where the light from the AGN is much stronger than the total disk and bulge contribution.

Lastly, the classification of galaxy as a starburst is based on a comparison with an IRAS sample of interacting galaxies and starburst models by Lehnert and Heckman (1996). Even highly reddened starburst systems are easily distinguished for ellipticals in multi-color diagrams such as  $vz - yz$  versus  $bz - yz$  (see RMS96). However, the tail end of the spiral sequence, composed of the late-type spirals, overlaps the starburst region. Again, from the point of view of a classification system aimed at the underlying stellar population, this simply acknowledges the fact that many late-type spirals have SFRs high enough to warrant a starburst classification. Thus, we emphasize that our scheme is not morphological and a majority of galaxies with Sc or Sd appearances would have a photometric classification of starburst in our scheme.

To increase the reliability of photometric classification, particularly for those galaxies whose colors place them at the borders of two different classifications, we have explored using data from nearby galaxies as template colors and assigning classification based on a statistical match in all four colors ( $mz$ ,  $uz - vz$ ,  $vz - yz$ ,  $bz - yz$ ). To this end, 132 spectrophotometric scans were extracted from the literature as outlined in Rakos, Maindl and Schombert 1996. The templates are selected from four catalogs: 1) elliptical/S0 (Gunn and Oke 1975), 2) normal spirals (Kennicutt 1992), 3) Markarian (De Bruyn and Sargent 1978) and an 4) IRAS sample (Ashby, Houck and Hacking 1992). All four of these catalog samples are shown in Figure 2. The division for the IRAS sample is particularly striking considering the sample was selected solely for far-IR color. IRAS galaxies with merger signatures (disturbed morphology, tidal features) are indicated by the solid symbols, but do not distinguish themselves from the other IRAS galaxies, probably an indication that dynamical features have much shorter timescales than star formation effects (Sanders *et al.* 1988). The Markarian sample is a good example of the degree of difficulty in classification when there is a mixture of non-thermal and disk colors as discussed above. In this case, there is a clear extension of the Markarian colors to anomalous  $bz - yz$  values for constant  $mz$ , but the overlap with normal spirals is problematic. In the overlap region, classification as a spiral is preferred in order to trace the global star formation history of the galaxy, rather than the evolution of the nuclear region. The spiral sequence neatly

divides into early and late-types, with early-types encroaching on the elliptical region and extreme late-types displaying starburst colors, again, reflecting the emphasis on star formation effects rather than dynamical or morphological appearance.

The multi-color, rest frame nature of our datasets have allowed for a fairly accurate classification of distant cluster members by photometric means since no k-corrections are involved. No single multi-color diagram (such as Figure 2) can portray all the information contained in the full photometry for each galaxy. Particularly for galaxies in the border regions, small errors in a single color can produce an erroneous classification. In order to minimize these errors, photometric class is assigned by a statistical weighting with respect to the template data. The templates are the same galaxies used in RMS96, only now weighted for all their colors (see Steindling, Borsch and Rakos 2000 for further discussion). The distant cluster data is directly compared with the template data and classification used herein is assigned based on the closest match. The difference between this method and simply using the divisions sketched RMS96 are minor, but this statistical method allows for some estimate of the internal errors of classification.

#### 2.4. A115

A115 is a binary cluster (Beers, Huchra and Geller 1983), our CCD survey centered on the southern component. The field of view does not include the northern component, so the data should be considered a study of only one subcluster in A115. Over 300 objects in the A115 fields were detected in all the four filters. For final analysis, a photometric selection criterion of cluster membership was applied such that an object must have an internal accuracy of  $\sigma < 0.07$  mag to be included. This resulted in a total of 100 cluster members. The classification fractions for both the blue and red populations are listed in Table 2. A115 was also studied on one of the original papers of this series (Rakos, Fiala and Schombert 1988). The current sample triples the number of galaxies with narrow band photometry for A115 from our original work, and the accuracy is improved such that we can now sample below  $L^*$ . The external errors were less than 0.01 for the lowest luminosity galaxies, and the mean color of the cluster is now  $vz - yz = 0.527$  compared to the old value of 0.529.

Figure 3 presents the  $vz - yz$  versus  $bz - yz$  and  $mz$  diagrams for the 100 cluster members. The various symbols display the photometric classifications based on template comparisons. The solid line in the left panel Figure 3 displays the relationship for normal spirals (Rakos, Maindl and Schombert 1997). Ellipticals and S0's have a slightly shallower correlation due to the color-magnitude relation (see §3.1). The starburst objects near the  $mz$  cutoff (blueward of  $vz - yz = 0.1$ ) probably represent starforming late-type spirals. The red starburst systems lie along the reddening vector, below the spiral sequence. Most of the starburst systems with  $mz < -0.25$  are low in luminosity (and, therefore, mass), and are the reddest of the non-elliptical objects in the sample. This starburst population is similar to the dwarf starburst population in A2317 (Rakos, Odell and Schombert 1997). The solid lines in the right panel of Figure 3 display the mean cutoffs for the population types, although comparison to templates is used for the final classifications as described in §2.2.

The population fractions are fairly normal for an intermediate redshift cluster. We find that 68 (68%) of the cluster members are type E/S0, whereas 11 (11%) are Sp/Irr, 17 (17%) are starburst and remaining 4 (4%) are classified as Seyfert galaxies. These ratios are slightly richer in early-type galaxies compared to the ratio for a nearby rich clusters, given as E:S0:Sp/Irr ratios of 20%:40%:40% (Oemler 1992). It is assumed that all the galaxies photometrically classified as Sp/Irr, starbursts and Seyferts would be morphologically

classified as late-type category. From this point of view, A115 is more evolutionary “developed” than A2317, meaning that it has a richer, red galaxy population and a weaker current star formation rate for the cluster as a whole. This is surprising given the dynamically young appearance to the A115 system as a whole (Beers, Huchra and Geller 1983). The fraction of Seyferts found in local clusters is extremely low, less than 1% of the total cluster population. However, a recent study by Sarajedini *et al.* (1996) finds the fraction of AGNs to increase to 10% between  $z = 0.2$  and 0.6. Thus, our observed value of 4% is in good agreement with expected number of AGNs at this epoch.

The blue fraction ( $f_B$ ) for A115 is 0.13 (again, we note that the values presented herein are for the southern subcluster only), where we maintain the original definition of blue populations from Butcher and Oemler (1984) as the number of galaxies 0.2 mag blueward from the k-corrected mean E/S0 color. In the Strömgren system, 0.2 mag from the E/S0 line translates into a rest frame blue/red cutoff of  $bz - yz = 0.2$ . This criteria will place many of the early-type spirals in the red category, although this would be expected from the dominance of the red bulge in such galaxies. However, a significant number of the starburst class galaxies will be misidentified as red population members due to heavy reddening by dust. As we will see below, many of the red starburst objects are low in luminosity and would not have contaminated the blue fraction values from earlier work of Butcher and Oemler (1984) or Dressler and Gunn (1983).

## 2.5. A2283

About 350 objects were measured in the 10 arcmin square field surrounding A2283. Elimination of foreground and background objects, stars and applying the photometric selection criterion for a minimal error of 0.07 mag, gives a total of 79 cluster members. The population fractions are listed in Table 3, such that 42 (53%) of the cluster members are E/S0, whereas 16 (20%) are Sp/Irr, 15 (19%) are classed as starburst and remaining 6 (8%) are classified as Seyfert or AGN galaxies.

Figure 4 presents the  $vz - yz$  versus  $bz - yz$  and  $mz$  diagrams for the 79 cluster members. Symbols and lines are the same as Figure 3. As can be seen in the figure, A2283 has a broader population of spirals as compared to A115. There is slightly more scatter about the spiral relation, having colors blueward about 0.1 mag for their  $vz - yz$  colors. This is probably due to weak AGN colors contaminating any otherwise pure disk population. The bluest starburst systems are redward of the spiral sequence along the reddening vector. The slope of the elliptical/S0 population in the  $vz - yz$ ,  $bz - yz$  plane is the same as A115.

The population of A2283 is richer in Sp/Irr and starburst galaxies compared to A115. We find that 39 (49%) of the cluster members are type E/S0, whereas 21 (27%) are Sp/Irr, 17 (22%) are starburst and remaining 2 (2%) are classified as Seyfert galaxies. This is slightly more spiral-rich than the nearby cluster morphological ratios, assuming that the starburst systems would be classed as late-type galaxies. The fraction of blue to red galaxies is 30% ( $f_B = 0.30$ ), high compared to A115 but similar to A2317 (Rakos, Odell and Schombert 1997). For this reason, we refer to A115 (and A2218) as red clusters and A2283 and A2317 as blue clusters. Again, the blue galaxies dominate the very bright and very faint end of the luminosity function and are located primarily at the cluster edges, which also mimics the behavior of A2317.

## 3. DISCUSSION

### 3.1. Cluster Population Fractions

The results of the photometric classification for A115 and A2283 are shown in Figures 3 and 4 and summarized in Tables 2 and 3. The distribution of the three primary galaxy types (ellipticals/S0s, spiral/irregular and starburst), as a function of magnitude, are also shown in Figure 5 for the combined populations of A115, A2283 and A2317. Although the three clusters differ in the fraction of their blue, red and starburst populations, all three follow the same behavior with respect to population type and luminosity. The ellipticals/S0 population have numerical superiority in all three clusters and have a distribution of luminosity that is typical for rich cluster of galaxies (Dressler *et al.* 1999). In contrast, the photometrically classified spirals/irregulars have a sharply different distribution, peaking at high luminosities ( $M_{5500} \approx -21$ ) and falling off to fainter magnitudes. The galaxies classified by our photometric scheme as starburst display the opposite behavior, rising to become a majority of the cluster population below  $M_{5500} = -21$ .

Where the behavior for the different photometric types in A115, A2283 and A2317 seems contrary to our expectations from studies of nearby clusters (i.e. that ellipticals and S0's dominate the bright end of luminosity function), it is not surprising when we remember that this is a photometric classification scheme. The objects in the spiral/irregular category may not be morphologically disk galaxies. Their classification is only a measure of the recent star formation history. In fact, the same luminosity distributions are evident in the Dressler *et al.* (1999) spectrophotometric catalog of ten distant clusters. Figure 7 of that paper displays the luminosity distribution for their sample divided by physical morphology and spectrophotometric class. The morphological distributions display the familiar cluster phenomenon of the bright end of the luminosity function being rich in ellipticals and S0's and late-type galaxies having lower mean luminosities. The number of spirals and irregulars is higher in the Dressler *et al.* sample compared to nearby clusters, and there are a larger number of bright, blue late-type galaxies (the Butcher-Oemler effect). The early-type galaxies still comprise a majority of the brightest galaxies. However, when the sample is divided by spectrophotometric class (where their  $k/k+a$  corresponds to our E/S0, e(a)/e(c) corresponds to our S/Irr and e(b) corresponds to our starburst class) then the luminosity distributions agree remarkably well with our Figure 5. Their e(a)/e(c) classes peak at  $M_{5500} = -23$  ( $H_o = 50 \text{ km sec}^{-1} \text{ Mpc}^{-1}$ ) and decrease in number, the same as our spiral/irregular class. Their e(b) class also follows the same behavior as our starburst population, a slow rise starting at  $M_{5500} = -22$ .

The differences between the characteristics of the three photometric populations can also be seen in Figure 6 where the fractions of the ellipticals/S0s, spiral/irregulars and starbursts galaxies are divided into four luminosity bins. The top panel displays the data for A2283 and A2317, the two clusters with high  $f_B$  values. The bottom panel displays the data for the red cluster, A115. Immediately obvious from Figure 6 is the fact that there are two competing contributions to the number of blue galaxies in all three clusters. At the bright end, one finds luminous objects with normal star formation rates which we classify photometrically as spirals/irregulars. As the contribution by this spirals/irregular population declines with luminosity, the fraction of starburst systems increases. This trend is common to both the red cluster (A115) and the blue clusters (A2283 and A2317). It seems clear from this figure that the Butcher-Oemler effect, the increase in  $f_B$  at these redshifts, is primarily due to the contribution of galaxies with spiral-like colors (i.e. normal star formation rates).

For further analysis of the changes in galaxy photometric type, we have divided the cluster members into three sub-populations; red, blue and starburst. The division between blue and red uses the same Butcher-Oemler criteria ( $bz - yz < 0.2$ ) as was used to determine  $f_B$  in each cluster. All objects classified as starburst, based on their  $mz$  index, comprise the starburst population. Over 98% of the galaxies classed

as elliptical/S0 (non-starforming) are members of the red population. The galaxies classed as Sp/Irr are evenly split between the red and blue populations (probably due to the effect that the early-type spirals by morphology comprise most of the red population Sp/Irr's). The starburst galaxies would also be fairly evenly split into blue and red types, if not separated into their own class. Each of these three sub-populations will be examined in the next sections.

### 3.2. Red Population

One of the dilemmas associated with the discovery of the Butcher-Oemler effect is that a majority of the present-day cluster population is composed of old, red objects (ellipticals and S0s) with effectively no recent SFR. However, a large number of the cluster galaxies at intermediate redshifts are involved in star formation at relatively high levels. The mystery, then, revolves around whether the blue population individuals are converted into red members with time or whether blue cluster members fade from view with time (or destroyed), boasting the ratio of red galaxies. All indications, from studies of the age and star formation history of present-day cluster ellipticals (Abraham *et al.* 1999, Buzzoni 1995) and the color evolution of the red population to redshifts of 1 (Rakos and Schombert 1995), are that the history of ellipticals is one of passive evolution from an epoch of formation near a redshift of 5. Where there may be transitions at intermediate redshifts of blue S0's into red S0's (as gas is depleted from star formation, see discussion below), a majority of the red population must have its origin from galaxies who have undergone an initial burst of star formation followed by passive evolution and, thus, should not be a member of the blue population at redshifts of 0.4.

This being the case, the red population provides an opportunity to examine age and metallicity predictions as a function of time. The most obvious test is to explore the mass-metallicity relationship of the red population as reflected in the observed color-magnitude diagram. In the closed-box models of galaxy evolution (Faber 1973; Tinsley 1980), the greater the mass of a galaxy (higher luminosity), the higher its supernova rate which results in a more rapid initial enrichment of the first generation of stars. This, in turn, produces a redder red giant branch (RGB) for the composite population and strong signatures in the  $vz - yz$  indices. The  $vz$  filter is located directly over several strong metal lines in an old population spectrum (Ca H and K, G band and Mg). Thus, there is the expectation that the  $vz - yz$  colors should be more sensitive to metallicity changes than most broadband indices. According to Visvanathan and Sandage (1977), the color magnitude relation is nearly zero from 5000 to 7000Å and increases steadily shortward of 4300Å reaching a maximum value of 0.11 mag per mag near 3400Å. The characteristics of metallicity and the Strömgren colors used here was studied extensively in Schombert *et al.* (1993) which found, and was confirmed by spectrophotometric models, that the  $vz - yz$  color was the strongest metal indicator for old stellar populations (i.e. ellipticals and S0's) of the  $uz, vz, bz, yz$  indices, and will be used for our color-magnitude analysis.

The  $vz - yz$  color-magnitude relation is shown in Figure 7 for the red populations in A115 (68 objects) and A2283 (39 objects) along with a linear fit. For this test, only the members of the red population classified as ellipticals/S0s are used and, despite the radically different population fractions between the two clusters, there is no statistically significant difference in the color-magnitude relation between the two clusters. Also plotted in Figure 7 is the red population data for A2317 (Rakos, Odell and Schombert 1997) along with the color-magnitude relation for present-day ellipticals from Schombert *et al.* (1993). The A2317 data is a excellent match to the present-day color-magnitude relation ( $\Delta(vz - yz)/\Delta(M) = -6.6 \times 10^{-2}$ ), but the data from A115 and A2283 is a factor of three shallower in slope ( $-9.8 \times 10^{-3} \pm 1.2 \times 10^{-2}$  and  $4.5 \times 10^{-3} \pm 1.6 \times 10^{-2}$  respectfully). While there is agreement at the low luminosities, the A115 and A2283

data do not redden as strongly as the A2317 data for increasing luminosity. This discrepancy does not appear to be due to errors in the observations. The A2317 data is of similar accuracy as the A115 and A2283 data, plus the shallow slope does not appear to be due to increased scatter at the low luminosity end. In fact, the brightest galaxies in both clusters display an unusual amount of scatter in  $vz - yz$  for their luminosity, despite the fact that their errors are the smallest. Thus, we conclude that the differences in the red populations are intrinsic to the clusters.

Closer inspection of the color-magnitude diagrams for A115 and A2283 shows that A2283 has a similar distribution as A2317, but with a larger scatter that lowers the slope as calculated from a regression fit. A115, on the other hand, clearly has a large number of bright galaxies, classified photometrically as ellipticals/S0s, with colors that are too blue for their luminosity, lying both below the red population in A2317 and below the relationship derived from present-day ellipticals. It should be noted that A115 has several galaxies that are in excess of the brightest cluster members of either A2283 or A2317 which contribute heavily to this effect.

While it would be interesting to speculate that the shallower slope in the color-magnitude relation is due to some evolutionary effect, comparison to models (Buzzoni 1995) indicates that subtle changes in the underlying stellar population dominate over metallicity effects at this epoch. For example, the contribution from horizontal branch (HB) stars peaks at these redshifts for a galaxy formation epoch between 5 and 10 (see Rakos and Schombert 1995). The HB sub-population has a brief dominant phase in the integrated colors, with an change of 0.1 mag in  $vz - yz$  color at redshifts of 0.4 (Charlot and Bruzual 1991), that would serve to lessen the strength of integrated mass-metallicity effect as only a narrow slice of stellar mass function is sampled rather than the whole RGB population. And this effect would be amplified if the HB sub-population has a range of metallicity producing blue to red HB stars, or if mergers with dwarf, metal-poor galaxies, also containing blue HB stars, has occurred in the recent past for the brighter cluster galaxies (i.e. galaxy cannibalism). This HB effect was seen in the color with redshift plots of Rakos and Schombert (1995) and would seem to be our best candidate to explain the larger range in colors for the A115 and A2283.

An alternative explanation is that the greater scatter in  $vz - yz$  color is due to contamination by blue S0's. These would be S0's which have recently (in the last 3 to 4 Gyr's) depleted their gas supplies and are evolving towards elliptical-like colors. The timescale for such a transition from spiral to S0 is evident in the near-IR colors of S0 disks (Bothun and Gregg 1990), and the brightest blue galaxies (classed as Sp/Irr in our scheme) would be obvious progenitors to these objects. In any event, it appears that, in the same manner as the blue population fraction of the Butcher-Oemler effect is irregular from cluster to cluster, the color-magnitude relation of the red population vary dramatically at intermediate redshifts and will require additional spectrophotometric information before any conclusions can be reached.

### 3.3. *Blue Population*

One advantage of the Strömgren colors (or any 4000Å color system) is the strong dependence of its indices on recent star formation and their sensitivity to recent deviations in star formation rates that signal starburst activity. RMS96 outlines the *uvby* system sensitivity to star formation effects using the starburst models of Lehnert and Heckman (1996, see Figure 6 of RMS96). Starforming galaxies cover a range of colors from blue to red with the more extreme starbursts located on the reddened side of the two color diagram. For the sake of consistence with previous work, we have maintained our past definition of  $f_B$ , the blue fraction in a cluster, based on a rest frame cut at  $bz - yz < 0.2$  regardless of extinction effects. While this criteria may

miss a substantial number of reddened starburst systems, thus reducing the meaning of  $f_B$  with respect to a clusters star formation history, we can isolate that population with other indices and discuss them separately (see §3.4).

The fraction of blue galaxies ( $f_B$ ) in A115 is  $0.13 \pm 0.04$ , whereas the  $f_B$  value for A2283 is  $0.30 \pm 0.06$ . This range is not unexpected as clusters located at intermediate redshifts display a wide variance of  $f_B$  values (from 0.11 in CL0024.5+1653 to 0.65 in A227, Rakos and Schombert 1995). In fact, the Butcher-Oemler effect is better described as the increased occurrence of blue populations with redshift, not a uniform correlation with redshift (Allington-Smith *et al.* 1993). As noted by the original Butcher-Oemler papers, there exist several distant clusters with quite red mean cluster colors, meaning similar to present-day clusters population fractions.

The  $f_B$  value in A2283 is similar to A2317 (Rakos, Odell and Schombert 1997) in that the blue population is strong at  $f_B = 0.30$ . Also similar to A2317, the blue population in A2283 displays a clear dependence on absolute magnitude such that blue galaxies dominate the very bright and very faint end of the luminosity function. As discussed in §3.1 and shown in Figure 6, the blue population at the high luminosity end is comprised mostly of galaxies photometrically classified as spirals/irregulars with an increasing contribution by starburst systems at low luminosities. Since early detections of the Butcher-Oemler effect were based on samples heavily weighted towards the bright galaxies, we can reliably state that the Butcher-Oemler effect, and therefore most of the blue population, is due to galaxies with normal star formation rates ( $\text{SFR} < 1 M_\odot \text{ yrs}^{-1}$ ). In clusters with a high  $f_B$  values (such as A2283 and A2317), there is a minor blue component from low luminosity starbursts, but this population has little impact on the calculated values of  $f_B$  since a majority of those systems are heavily reddened.

The blue population in A2317 was found to have a wider distribution of radii then the red population (see Figure 6 in Rakos, Odell and Schombert 1997). Figure 8 displays the same analysis for A2283 and demonstrates that the same effect is also found there (the blue population in A115 was too small for a robust statistical test). The difference in the radial distribution of the blue population is even more extreme in A2283 than A2317, having a peak at 0.5 Mpc from the cluster center. This result remains regardless if the cluster center is calculated using geometric cluster center, the x-ray center or the center defined by the brightest cluster galaxy. Figure 8 also shows that the red population in A2283 is strongly peaked at the center with a core density of 160 galaxies per  $\text{Mpc}^2$ . The blue population, on the other hand, are deficient in the cluster core, located primarily in the outer regions of the cluster.

As discussed in Rakos, Odell and Schombert 1997 for the A2317 data, a mechanism for cluster induced star formation has been proposed by Moore *et al.* (1996) called galaxy harassment which emphasizes tidally induced star formation imposed by both the mean cluster tidal field and rapid impulse encounters with massive galaxies at the cluster core. One of the predictions of galaxy harassment is that galaxies in the cores of clusters will be older than galaxies at the edges. In terms of star formation history, this is the behavior seen in Figure 8 for A2283 and A2317. The blue population (i.e. the harassed population) is primarily located in the outer 2/3's of the cluster. Other explanations, such as infall of spiral-rich subclusters, are unsupported since the blue population is not clumped nor confined to the edges of the cluster.

We arrive at the conclusion that each of the clusters studied herein seem to be composed of two distinct components in terms of star formation history. The scenario for the construction of the blue population proposed here is similar to the one we proposed in RS95, that the Butcher-Oemler population is an evolved set of gas-rich (possibly low in surface brightness) galaxies. The mechanism of galaxy harassment induces highly efficient star formation in these dark matter dominated systems that increases their luminosity and

visibility. Later encounters with the cluster core destroy these low density systems by tidal forces, effectively removing them from the present-day cluster sample. Eventually, the Butcher-Oemler clusters at intermediate redshifts will evolve into future cD clusters from the released stellar material of the disrupted blue population.

Lastly, we consider the Seyfert-like galaxies in A115 and A2283. Although the number of Seyferts is slightly above normal (as compared to nearby rich clusters), they are by no means a major component of the Butcher-Oemler effect. The amount of AGN activity certainly increases with redshift for cluster populations (Sarajedini *et al.* 1996) and the number of galaxies classified as Seyferts in this data set is in agreement with those studies even though we believe our classification to be extremely conservative. Whether the increase in the number of Seyferts is related to the increase in the blue population with redshift (the Dressler-Gunn effect) or whether this is a parallel processes remains undetermined by this dataset. A worthwhile future study would be high resolution spectroscopy of the Seyfert objects and many of the high  $mz$  spiral/irregulars as a probe to the range and strength of AGN's in Butcher-Oemler clusters.

### 3.4. Starburst Population

The behavior of starburst galaxies for the  $uz, vz, bz, yz$  color system was investigated in RMS96 by analysis of a set of interacting and merging galaxies. In that paper, it was demonstrated that it is possible to differentiate between starburst galaxies shrouded in dust with strong reddening (IRAS starbursts, Lehnert and Heckman 1996), versus the strong ultraviolet radiation of Wolf-Rayet galaxies, simply by the distance the galaxy lies from the spiral/irregular sequence along the reddening vector, although the exact amount of reddening is difficult to determine due to its shallow slope. The reddening line (see Figures 3 and 4) indicates that a majority of the starburst galaxies from the IRAS sample have Sb or later colors with significant extinction ( $A_V > 5$ ) by dust, in same range as IRAS starbursts (Leech *et al.* 1989).

Despite the difference in the blue fractions of A115 and A2283, their starburst populations are similar at 17% and 22% respectfully (A2317 also has a 22% starburst fraction). Both clusters starburst population are heavily weighted toward the faint end of the luminosity function, as was the starburst population in A2317. The starburst galaxies are evenly divided between the blue and red populations, reflecting the frequent occurrence of heavy dust extinction since the blue starbursts lie on the spiral sequence and the red starbursts lie in the reddened portion of the two-color diagrams. For example, most of the blue population in A115 is due to starburst galaxies since there is a real deficiency in spiral/irregular class objects. In contrast, the blue population in A2283 is comprised evenly of both spirals/irregulars and starbursts.

The luminosity distribution indicates that the starburst population entails a phenomenon that is focused on the faint galaxies in a cluster. While some of the starburst systems are quite luminous, comparable to Arp 220 in the strength of their current star formation, most are of low total luminosity even while, apparently, at the peak of their star formation rates. This is in sharp contrast with an IRAS selected local sample of galaxies (Kim and Sanders 1998) where a majority of those systems are extremely luminous and massive. The cluster starburst population appears to be composed of a unique type of galaxy, possibly the progenitors of present-day dwarf ellipticals and BCD's. Deeper *Hubble Space Telescope* (HST) observations by Koo *et al.* (1997), Oemler *et al.* (1997) and Couch *et al.* (1998) have shown that many of the starbursts in distant clusters tend to be small objects whose final state is likely to be just such a dwarf galaxy. Further support for this view comes from the observations that dwarf galaxies in Virgo, Fornax and Coma have undergone recent episodes of star formation in the last 4 to 5 Gyrs (Bothun and Caldwell 1984), which corresponds to the epoch of the starburst population in all three of the intermediate redshift cluster we have studied.

#### 4. CONCLUSIONS

The trends with respect to cluster populations for A115 (southern subcluster) and A2283 (combined with the data for A2218 and A2317) are shown in Figure 9. The data for A2317 are published in Rakos, Odell and Schombert (1997) and the data for A2218 will be published in Rakos, Dominis and Steindling (2000). Four parameters are plotted with respect to the elliptical/S0 fraction; the fraction of the blue population ( $f_B$ ), the fraction of starburst galaxies, the richness of the cluster ( $C$ ) and the radius of where the maximum value of  $f_B$  occurs.

The fraction of the blue population drops inversely with the E/S0 percentage. This is not too surprising since a majority of the red population is classified photometrically as E/S0's. However, the relation is nearly 1-to-1, suggesting that it is conversion of the E/S0 objects into the blue population that comprises the Butcher-Oemler effect. Since our previous work on present-day ellipticals and the color evolution of ellipticals (Schombert *et al.* 1993, Rakos and Schombert 1995) demonstrates that their colors have a narrow range and closely match the models for a passively evolving population with a formation redshift of 5, we must conclude that it is primarily the S0 galaxies that are the normal starforming objects of the Butcher-Oemler population. This scenario matches well to our expectations of gas depletion, where large bulge S0's exhaust their supply first, followed by Sa's, then Sb's in the near future. We can assume that a gas-rich, proto-S0 undergoing star formation rates of around  $1 M_\odot \text{ yrs}^{-1}$  will produce spiral structure and have morphologies similar to early-type spirals as revealed by HST imaging.

The fraction of starbursts is only weakly related to the E/S0 fraction confirming the split impact that the reddened starburst galaxies have on the color distribution of cluster populations. This is a new phenomenon for distant clusters and, while the same mechanisms may be at work for the dwarf starbursts, we believe this is a separate event from the Butcher-Oemler effect.

The radius of the peak density of the blue population is also uncorrelated with any population fraction or color fraction of the clusters. This fact is illuminating in the sense that distribution of the blue population in the red clusters (A115 and A2218) is similar to that of the blue clusters (A2283 and A2317). If tidal forces are responsible for the blue population, then there will be a mix of effects due to close encounters with other galaxies and the mean cluster tidal field which will only be weakly dependent on the cluster morphology. If ram pressure stripping is important, then this radius should be correlated with the x-ray profile of the cluster.

One of the primary results of this study is that there appears to exist a *duality* with respect to cluster population studies by morphology versus photometric classification. Morphological studies of intermediate redshift clusters (Oemler, Dressler and Butcher 1997, Dressler *et al.* 1997) find the fraction of ellipticals to be similar to present-day clusters with a sharp drop in the number of S0's and a proportional increase in the number of spirals and irregulars. There is also an increase in the number of disturbed galaxies with redshift (Couch *et al.* 1998), galaxies with tidal signatures of past encounters. On the other hand, photometric classification (such as this study and Dressler *et al.* 1999) find a population of bright blue galaxies with normal star formation rates (the Butcher-Oemler effect) and a starburst population, dominated by low mass galaxies. But, the characteristics of these populations differ in their luminosity and geographical distributions compared to their morphological counterparts. This is particularly evident in magnitude diagrams such as Figure 5 compared to similar diagrams for nearby, rich clusters. *The underlying consequence of this duality is the decoupling of the presence of star formation of the properties of Hubble types with redshift* (i.e. the existence of blue S0's, starbursting dwarfs, disturbed spirals at high redshift).

How this decoupling takes place is due to a separation of formation events (such as the density of the protogalaxy, the fraction of dark to baryonic matter) and the later effects of environment. Clearly, local density plays an important role in the evolution of a galaxy. As shown in Hashimoto *et al.* 1998, galaxies at intermediate densities have higher star formation rates than galaxies located in high dense regions (such as the core of a rich cluster). If the dominate process were galaxy encounters that induce star formation, then this correlation would be expected as intermediate density environments (such as loose groups) have the appropriate mix of galaxy density and low velocities to maximize tidal effects (Hashimoto *et al.* 1998). However, a competing process, that a pure density analysis does not take into account, is the possibly of ram pressure effects from the hot intracluster gas identified with every rich cluster of galaxies. There is clear evidence of such stripping ongoing in nearby clusters, such as Virgo, based on the HI and CO images of cluster spirals (Kenney and Young 1989).

We conclude that the Butcher-Oemler effect in rich clusters is the phenomenon of starforming S0's being ram pressure stripped as they encounter the hot gas in the core of the cluster. The elimination of the atomic gas prematurely ceases star formation (although the question remains of the interplay with the molecular gas) and the S0's disks age to the population we see today. On the other hand, the dwarf galaxy interactions in the outer regions of the cluster (where the velocities are lower) produce the starburst population. Both the blue and starburst population avoid the core of the cluster, but each for different reasons, one being intrinsic, the other environmental.

The authors wish to thank the directors and staffs of KPNO, Steward and Wise Observatories for granting time for this project. Financial support from Austrian Fonds zur Foerderung der Wissenschaftlichen Forschung is also gratefully acknowledged. This research has made use of the NASA/IPAC Extragalactic Database (NED) which is operated by the Jet Propulsion Laboratory, California Institute of Technology, under contract with the National Aeronautics and Space Administration.

## REFERENCES

- Abraham, R., Ellis, R., Fabian, A., Tanvir, N. and Glazebrook, K 1999, MNRAS, 303, 641  
Allington-Smith, J., Ellis, R., Zirbel, E. and Oemler, A. 1993, ApJ, 404, 521  
Ashby, M., Houck, J. and Hacking, P. 1992, AJ, 104, 980  
Beers, T., Huchra, J. and Geller, M. 1983, ApJ, 264, 356  
Butcher, H. and Oemler, A. 1984, ApJ, 285, 426  
Bothun, G. and Caldwell, C. 1984, ApJ, 280, 528  
Bothun, G. and Gregg, M. 1990, ApJ, 350, 73  
Bothun, G. and Schombert, J. 1990, ApJ, 360, 436  
De Bruyn, A. and Sargent, W. 1978, AJ, 83, 1257  
Buzzoni, A. 1995, ApJS, 98, 69  
Charlot, S. and Bruzual, G. 1991, ApJ, 367, 126  
Couch, W., Ellis, R., Sharples, R. and Smail, I. 1994, ApJ, 430, 121  
Couch, W., Barger, A., Smail, I., Ellis, R., Sharples, R. 1998, ApJ, 497, 188  
Dressler, A. and Gunn, J. 1983, ApJ, 270, 7

- Dressler, A., Oemler, A., Butcher, H. and Gunn, J. 1994, *ApJ*, 430, 107
- Dressler, A., Oemler, A., Couch, W., Smail, I., Ellis, R., Barger, A., Butcher, H., Poggianti, B. and Sharples, R. 1997, *ApJ*, 490, 577
- Dressler, A., Smail, I., Poggianti, B., Butcher, H., Couch, W., Ellis, R., and Oemler, A., 1999, *ApJ*, 122, 51
- Faber, S., 1973, *ApJ*, 179, 731
- Fiala, N., Rakos, K. and Stockton, A. 1986, *PASP*, 98, 70
- Gunn, J. and Oke, J. 1975, *ApJ*, 195, 255
- Hamilton, D., 1985, *ApJ*, 297, 371
- Hashimoto, Y., Oemler, A., Lin, H. and Tucker, D. 1998, *ApJ*, 499, 589
- Ho, L., Filippenko, A. and Sargent, W. 1997, *ApJS*, 112, 315
- Kenney, J. and Young, J. 1989, *ApJ*, 344, 171
- Kennicutt, R. 1992, *ApJS*, 79, 255
- Kennicutt, R. 1998, *ApJ*, 541
- Kim, D. and Sanders, D. 1998, *ApJS*, 119, 41
- Koo, D., 1986, *ApJ*, 311, 651
- Koo, D., Guzman, R., Gallego, J., and Wirth, G. 1997, *ApJ*, 487, L49
- Leech, K., Penston, M., Terlevich, R., Lawrence, A., Rowan-Robinson, M. and Crawford, J. 1989, *MNRAS*, 240, 349
- Lehnert, M. and Heckman, T. 1996, *ApJ*, 472, 546
- Massey, P., Strobel, K., Barnes, J. and Anderson, E. 1988, *ApJ*, 328, 315
- Morgan, W. and Mayall, N. 1957, *PASP*, 69, 291
- Moore, B., Katz, N., Lake, G., Dressler, A., and Oemler, A. 1996, *Nature*, 379, 613
- Oemler, A., Dressler, A. and Butcher, H. 1997, *ApJ*, 474, 561
- Oemler, A. 1992 , in Clusters and Superclusters of Galaxies, ed. Fabian (Dordrecht:Kluwer), 666
- Oemler, A., Dressler, A., and Butcher, H. 1997, *ApJ*, 474, 561
- Oke, J. and Gunn, J. 1983, *ApJ*, 266, 713
- Moore, B., Lake, G., Quinn, T. and Stadel, J. 1999, *MNRAS*, 304, 465
- Poggianti, B., Smail, I., Dressler, A., Couch, W., Barger, A., Butcher, H., Ellis, R. and Oemler, A. 1999, *ApJ*, 518, 576
- Rakos, K., Fiala, N., and Schombert, J. 1988, *ApJ*, 328, 463
- Rakos, K., Schombert, J., and Kreidl, T. 1991, *ApJ*, 377, 382
- Rakos, K., and Schombert, J. 1995, *ApJ*, 439, 47
- Rakos, K., Maindl, T., and Schombert, J. 1996, *ApJ*, 466, 122 (RMS96)
- Rakos, K., Odell, A., and Schombert, J. 1997, *ApJ*, 490, 194
- Rakos, K., and Schombert, J. 1999, in The Evolution of Galaxies on Cosmological Timescales ASP Conference Series, ed. J.E. Beckman and T.J. Mahoney, in print

- Sanders, D., Soifer, B., Elias, J., Madore, B., Matthews, K., Neugebauer, G. and Scoville, N. 1988, ApJ, 325, 74
- Rakos, K., Dominis, D. and Steindling, S. 2000,  $\ddot{a}$ , in prep
- Sarajedini, V., Green, R., Griffiths, R., and Ratnatunga, K. 1996, ApJ, 471, L15
- Schombert, J., Hanlan, P., Barsony, M. and Rakos, K. 1993, AJ, 106, 923
- Steindling, S., Brosch, N. and Rakos, K. 2000, ApJ, submitted
- Tinsley, B. 1980, Fundam. Cosmic Phys., 5, 287
- Tyson, J. 1988, AJ, 96, 1
- Visvanathan, N., and Sandage, A. 1977, ApJ, 216, 214
- Wang, Q. and Ulmer, M. 1997, MNRAS, 292, 920

Fig. 1.— Two color diagrams and tracks for redshift effects. The shaded areas represent the regions occupied by ellipticals and spirals. The two tracks are the observed colors for a typical elliptical spectrum (NGC 3379) and a starforming spiral (NGC 6643) for redshifts ranging from  $-0.10$  to  $0.10$ . Background and foreground galaxies (beyond  $-0.05$  and  $0.05$  of the cluster mean) can be identified by their deviant color indices. Additional membership information from the  $vz - bz$  colors are not shown.

Fig. 2.— Two color diagrams for template galaxies. The two color indices,  $vz - yz$  and  $bz - yz$  (roughly  $4250\text{\AA}$  -  $5500\text{\AA}$  and  $4750\text{\AA}$  -  $5500\text{\AA}$ ) are shown for the four photometric classes based on template data discussed in RMS96. The solid line in each panel is the normal starforming sequence. The spiral templates are divided into Sa's (crosses), Sb (solid diamonds) and Sc's (squares). The starburst templates are divided into normal (solid diamonds) and interactions/mergers (crosses) based on disturbed morphology. As discussed in the text, the ellipticals and S0's form a distinct grouping in multi-color space at the red end. Spirals form a linear sequence with the early-type spirals (large red bulge) overlapping the E/S0 region and the late-type spirals overlapping the starburst region. Seyferts form a sequence above the spirals, indicating the contribution from a non-thermal component to their optical luminosity. The starbursts lie below the spiral sequence depending on the amount of reddening present.

Fig. 3.— Two color and  $mz$  diagrams for A115. The four photometric classes are displayed in the  $vz - yz$ ,  $bz - yz$  and  $mz$  planes. The solid line in the  $vz - yz$ ,  $bz - yz$  diagram is the spiral sequence from Figure 2. The solid lines in the  $vz - yz$ ,  $mz$  diagram demarcate the the classification boundaries from RMS96. A typical error bar for the faintest galaxies is shown. Although a majority of the galaxies are red, non-starforming systems, there are a significant number of bright, blue spirals (the Butcher-Oemler effect) as well as a low luminosity population of starburst galaxies.

Fig. 4.— Two color and  $mz$  diagrams for A2283. The four photometric classes are displayed in the  $vz - yz$ ,  $bz - yz$  and  $mz$  planes. Lines and symbols are the same as Figure 3. A2283 is a high  $f_B$  cluster. The diagrams show that a majority of the blue galaxies are normal starforming galaxies (spirals).

Fig. 5.— Luminosity distribution for the three primary population types in A115, A2283 and A2317. The composite luminosity histograms in the  $M_{5500}$  magnitude system (approximately Johnson  $V$ ) are shown for all three clusters. The ellipticals/S0s display typical luminosities for a rich cluster. However, the spirals/irregulars are strongly peaked at high luminosity indicating their dominant contribution to the Butcher-Oemler effect. The starburst galaxies display an opposite behavior, rising to a peak at low luminosities. Incompleteness is estimated to begin at  $M_{5500} = -19$ .

Fig. 6.— The population fractions for the blue clusters (A2283 and A2317) versus the red cluster (A115). The three primary population types (E/S0, spiral and starburst) are divided into 4 luminosity bins. The solid lines show the change in  $f_B$  with luminosity. Both blue and red clusters display similar traits with respect to the drop then rise of  $f_B$  and the rise of the fraction of starburst galaxies with decreasing luminosity, despite their differences in global population types. The blue population is dominated by normal starforming objects at high luminosity, with an increasing contribution from low mass starbursts.

Fig. 7.— The color-magnitude relation for the red populations in A115, A2283 and A2317. The various symbols display the metallicity color index,  $vz - yz$ , versus absolute magnitude,  $M_{5500}$ . The solid line is a linear fit to the A115 and A2283 data. The dotted line is from the relationship for present-day ellipticals (Schombert *et al.* 1993). While the scatter is high, the differences in the slopes of the three clusters is clear. The large range for the brightest red galaxies may be due to HB contributions to the integrated light, or blue S0's evolving into normal S0 colors.

Fig. 8.— The radial distribution of the blue and red populations for A2283. The blue and red populations are divided into four radial bins measured from the geometric cluster center. The blue population is clearly deficient in the cluster core and peaks 0.5 Mpc from the cluster center. The red population dominates the cluster core by number.

Fig. 9.— Summary of cluster properties for A115, A2218, A2283 and A2317. Four parameters are plotted with respect with respect to the E/S0 fraction for each cluster; the fraction of the blue population ( $f_B$ ), the fraction of starburst galaxies, the richness of the cluster ( $C$ ) and the radius of where the maximum value of  $f_B$  occurs.

Table 1. Clusters Properties

Cluster	RA (1950)	Dec	BM type	C	R	z	$f_B$	E/S0%	Starburst %	max $f_B$ radius
A115	0056.0+2619		III	174	3	0.197	0.13	67±8	17±4	0.45
A2218	1635.9+6612		II	214	4	0.171	0.23	65±7	10±3	0.50
A2283	1744.5+6938		I	65	1	0.183	0.30	49±8	22±5	0.55
A2317	1908.3+6903		II	186	3	0.211	0.35	42±7	22±4	0.30

Table 2. A115 Cluster Population

Type	Blue	Red	Total
E/S0	1 ( 8%)	67 (78%)	68 (68±8%)
Sp/Irr	1 ( 8%)	10 (11%)	11 (11±3%)
Sy/AGN	4 (20%)	0 ( 0%)	4 ( 4±2%)
Starburst	7 (54%)	10 (11%)	17 (17±4%)
Total	13 (13±3%)	87 (87±9%)	100

Table 3. A2283 Cluster Population

Type	Blue	Red	Total
E/S0	1 ( 4%)	38 (69%)	39 (49±8%)
Sp/Irr	11 (46%)	9 (16%)	20 (25±6%)
Sy/AGN	3 (13%)	0 ( 0%)	3 ( 4±2%)
Starburst	9 (38%)	8 (15%)	17 (22±5%)
Total	24 (30±6%)	55 (70±9%)	79

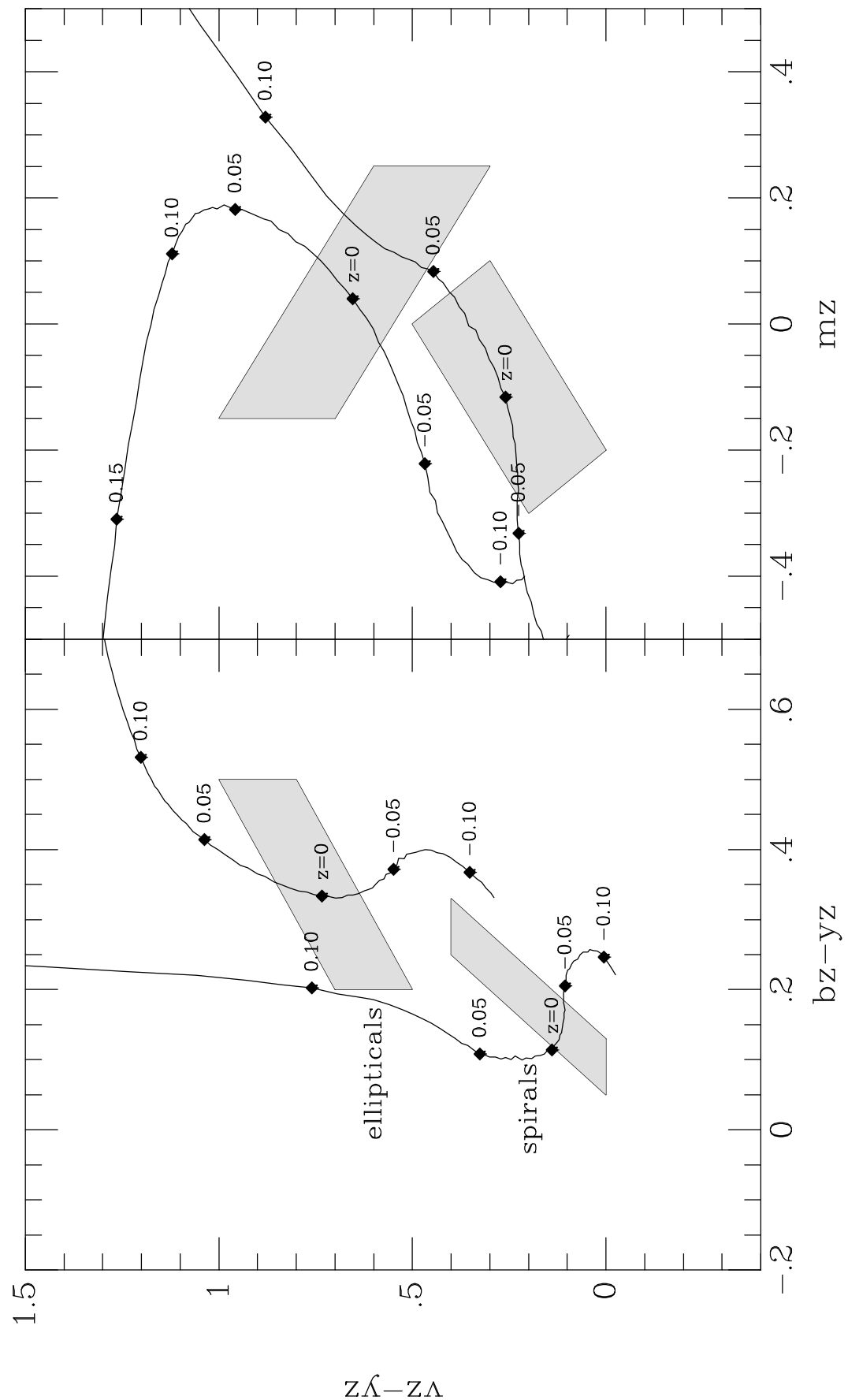


Figure 1

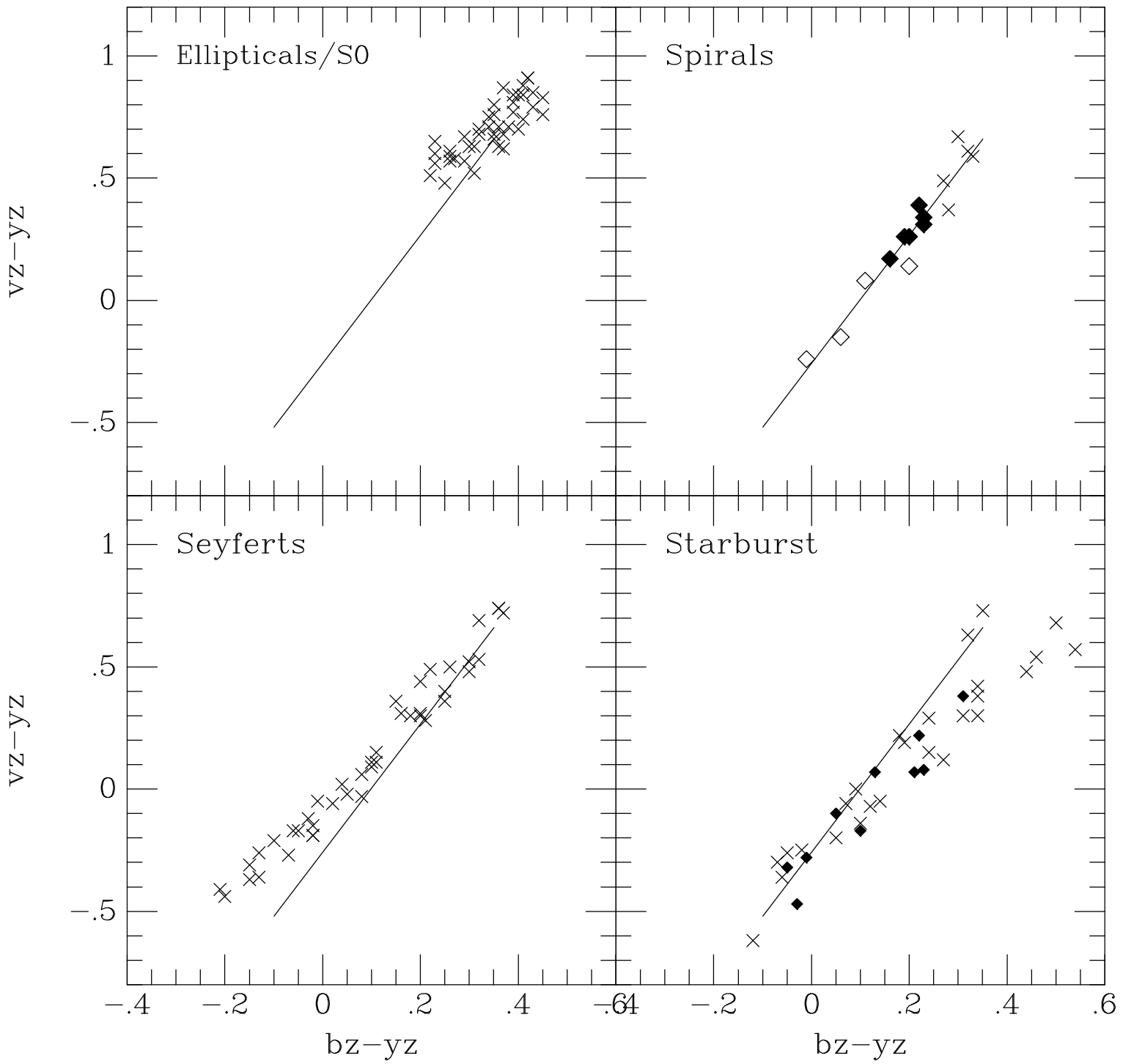


Figure 2

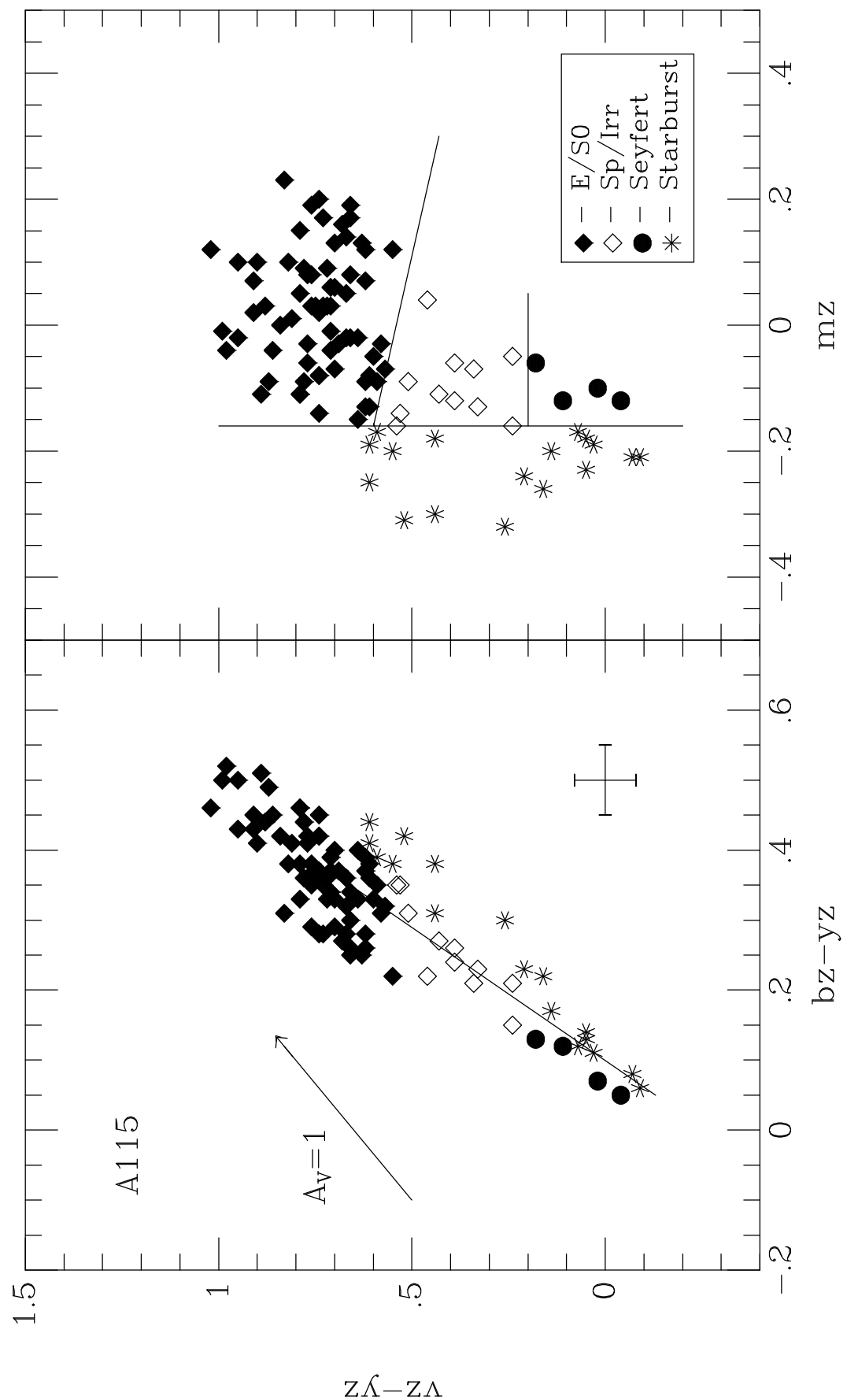


Figure 3

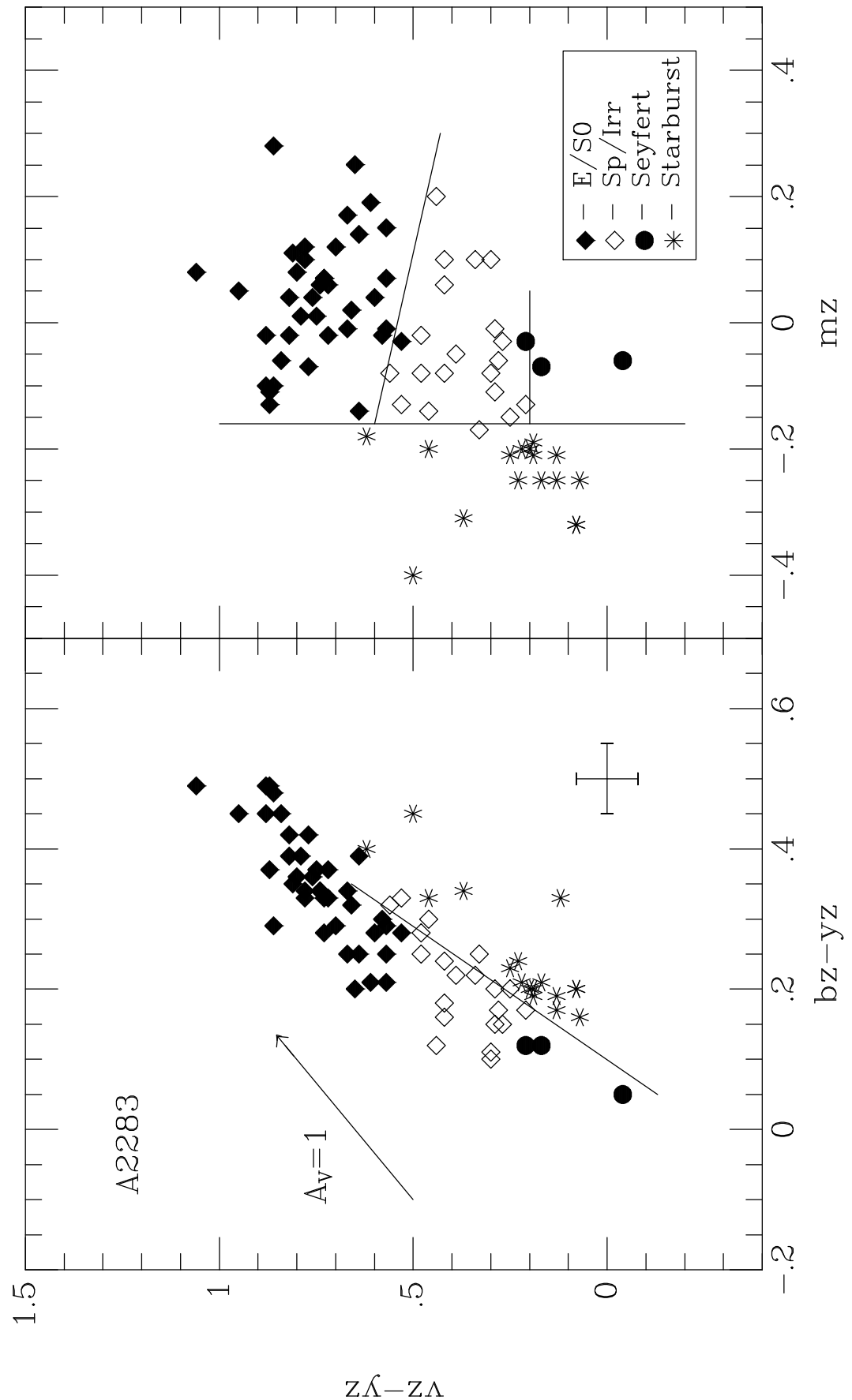


Figure 4

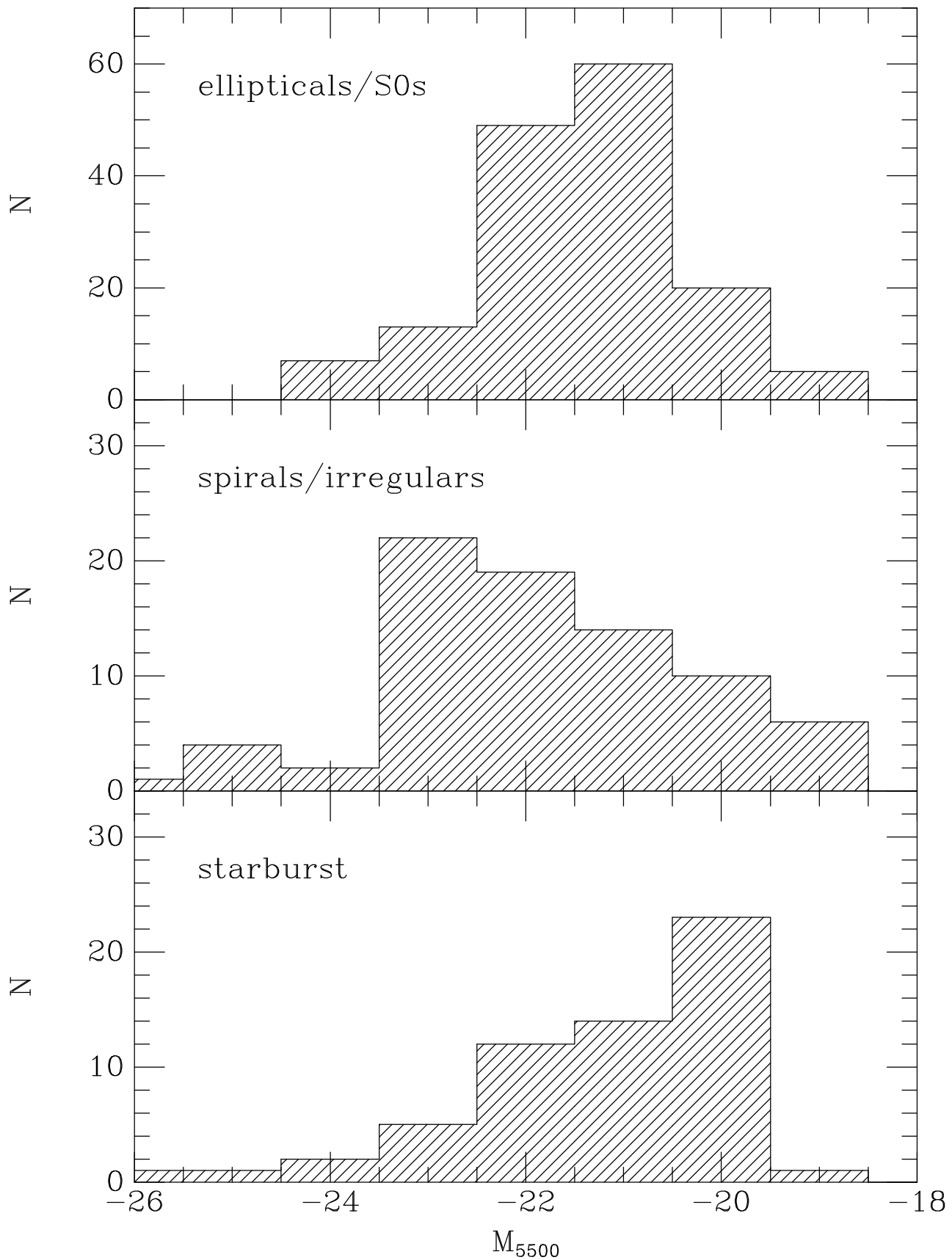


Figure 5

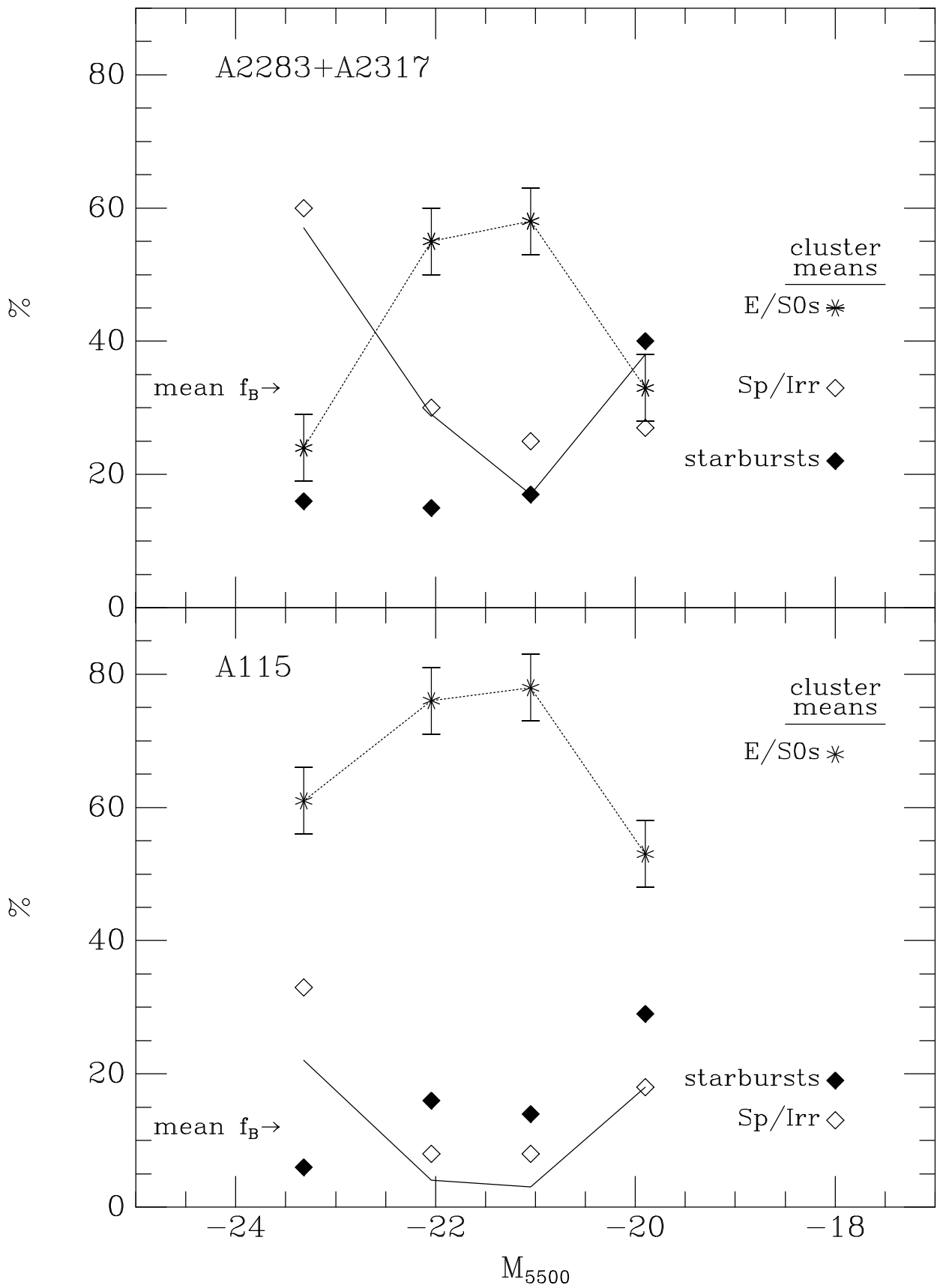


Figure 6

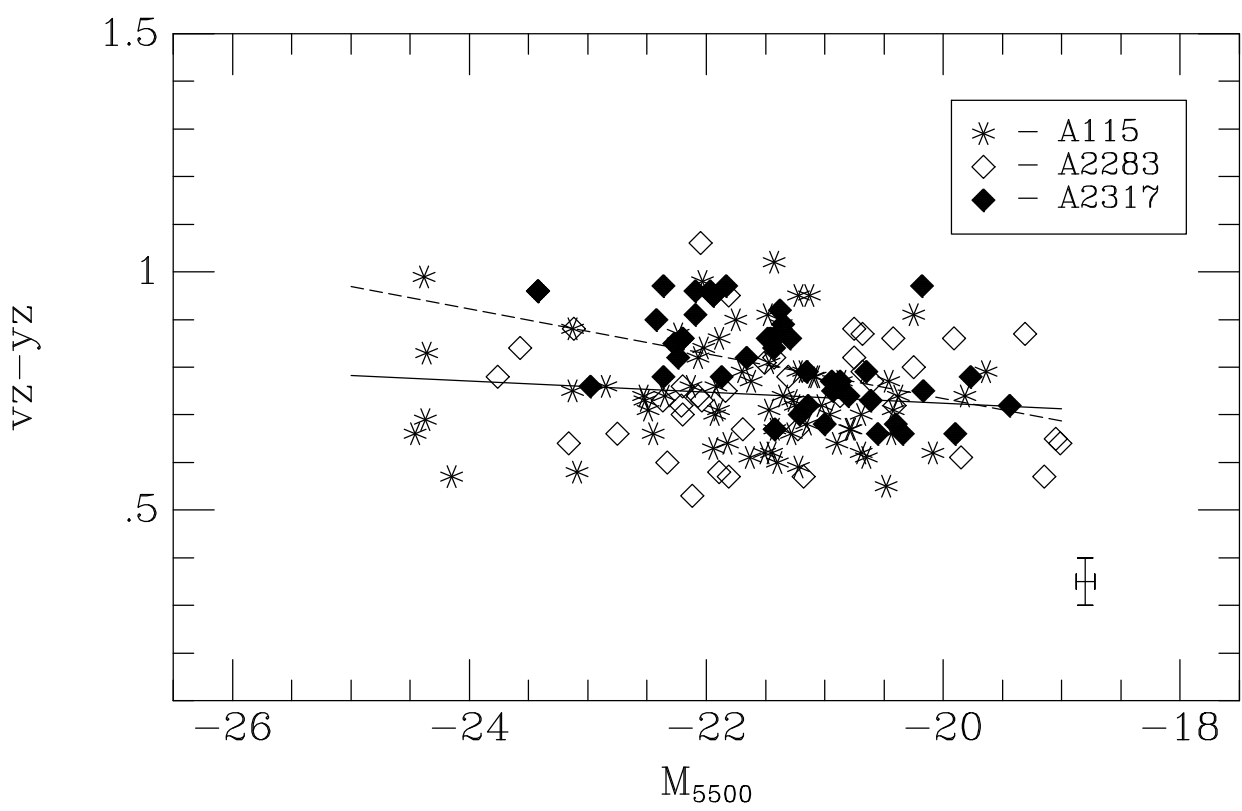


Figure 7

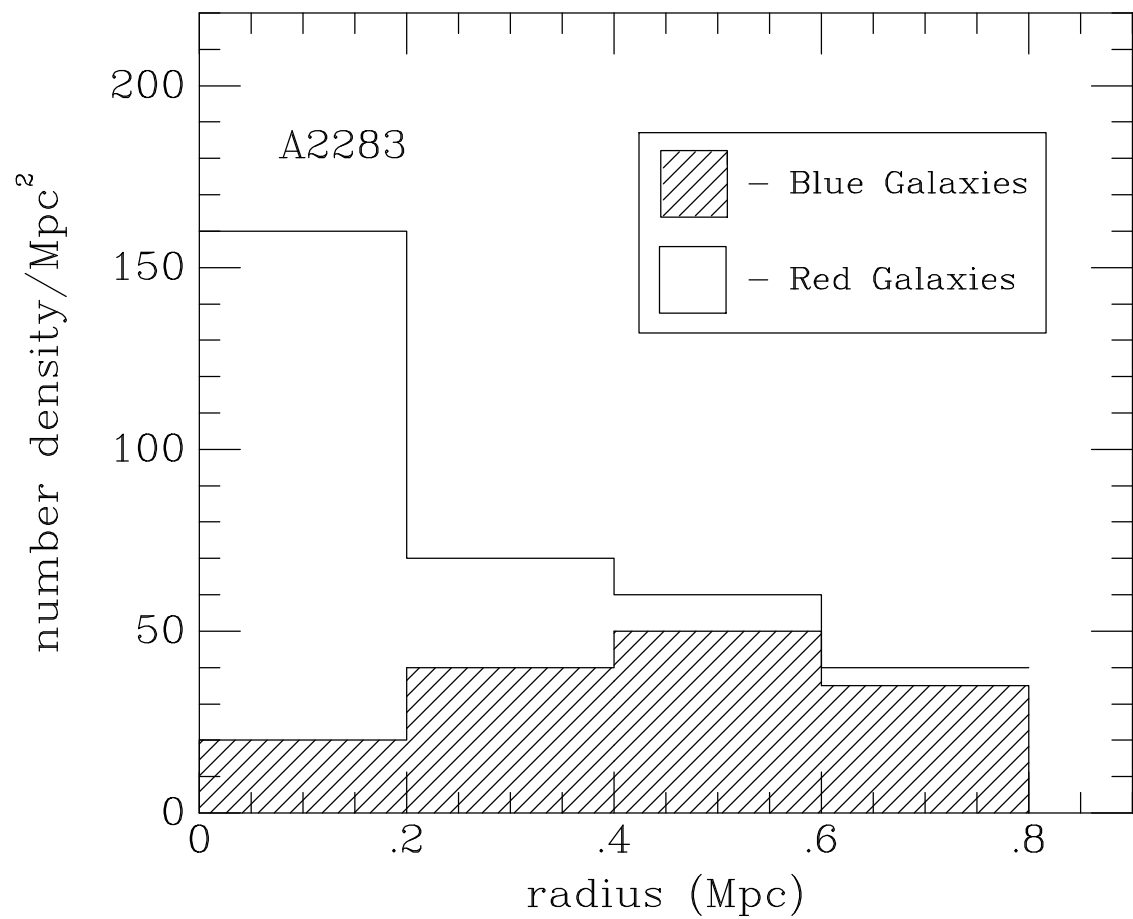


Figure 8

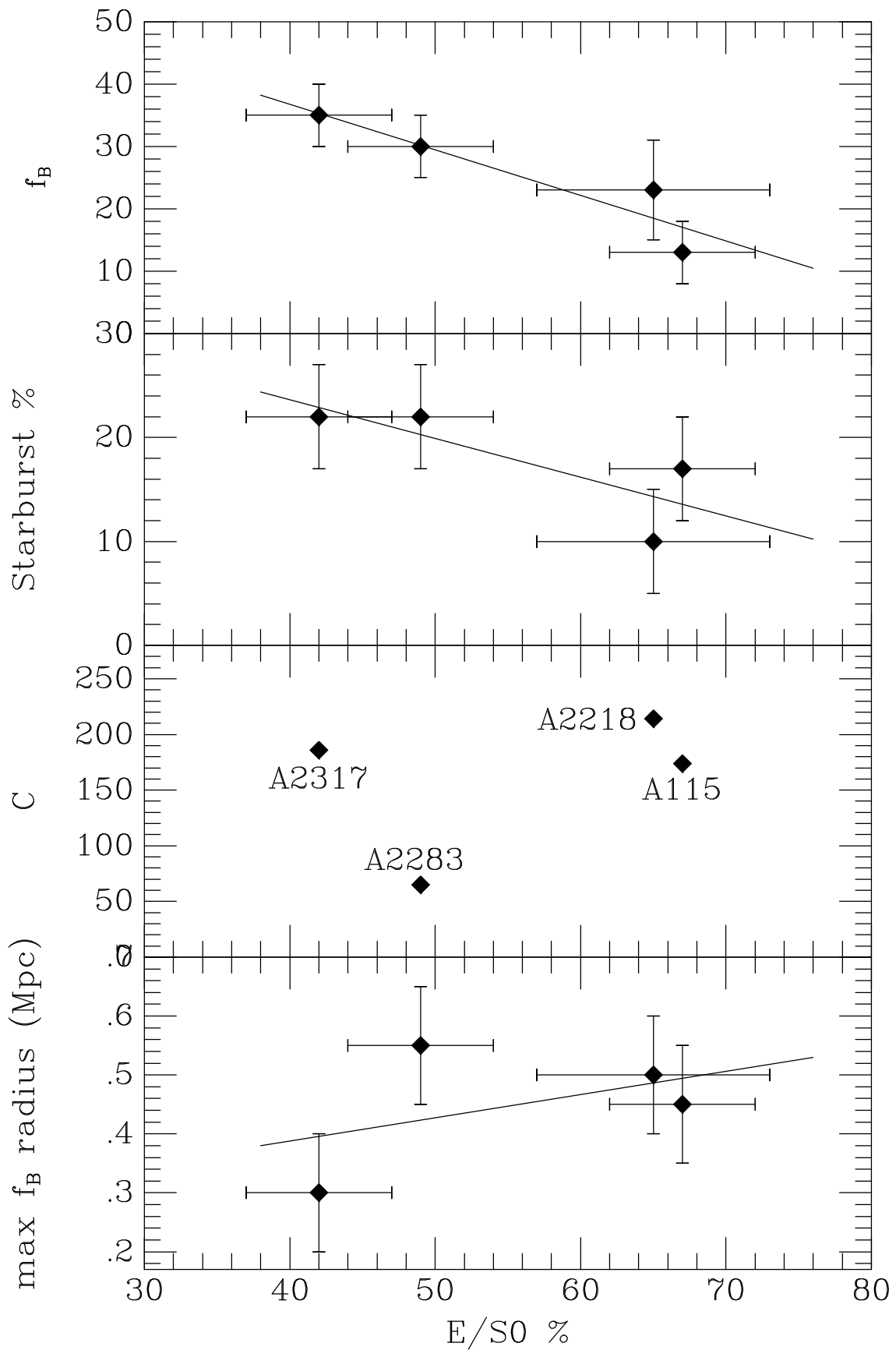


Figure 9